SAND2011-8346C

AIAA Reno Jan 2003, #0870

Modeling of blades as equivalent beams for aeroelastic analysis

by

David J. Malcolm
Global Energy Concepts, LLC

and

Daniel L. Laird
Sandia National Laboratories

Abstract

Introduction

The blades of a modern wind turbine are key components, central to all aspects of the system from energy capture to system dynamics to tower clearance. They are also complex structural items, typically comprising many layers of fiber reinforced material with necessary shear webs, root fixtures, and tapering cross sections. Special codes have been developed to construct 3-dimensional finite element models of such blades [Laird, 2001] typically using thousands of composite shell elements. These models are of value in examining the internal stress distribution within the blade but are too detailed for use in a system aeroelastic analysis which normally represents the blades as a series of 1-dimensional beam elements.

The 1-dimensional beam element must accurately represent all of the mechanical properties of the full 3-dimensional blade including shear deformation, coupling between the various forces and moments and the offsets of the elastic and shear centers. Attempts at capturing all of this information by examining the sections alone have been prone to approximations and omission of important aspects. To accomplish this task in a comprehensive manner, Sandia National Laboratories have funded a program of code development which is now near completion. There are three basic steps in the process established:

1. Create an ANSYS® [ANSYS Inc] finite element model through the NuMAD interface [Laird, 2001].
2. Apply a suite of unit tip loads and transfer the displacement results to a series of MATLAB® routines which extract the stiffness matrices for the equivalent beam elements.
3. Incorporate the stiffness matrices into a preprocessor and generate the complete aeroelastic model for the ADAMS® code [Mechanical Dynamics, 1994].

Global Energy Concepts LLC (GEC) has worked under contract to Sandia National Laboratories to develop the basic algorithms for this task and have carried out validation of the preliminary steps. This has been reported in detail in [GEC,2001] and [GEC,2002]. The purpose of this paper is to present an overview of the method and to report on the application of the procedure to complete blades and to wind turbine models.

Approach

A flowchart of the overall process, from selection of materials to final aeroelastic code, is shown in Figure 1

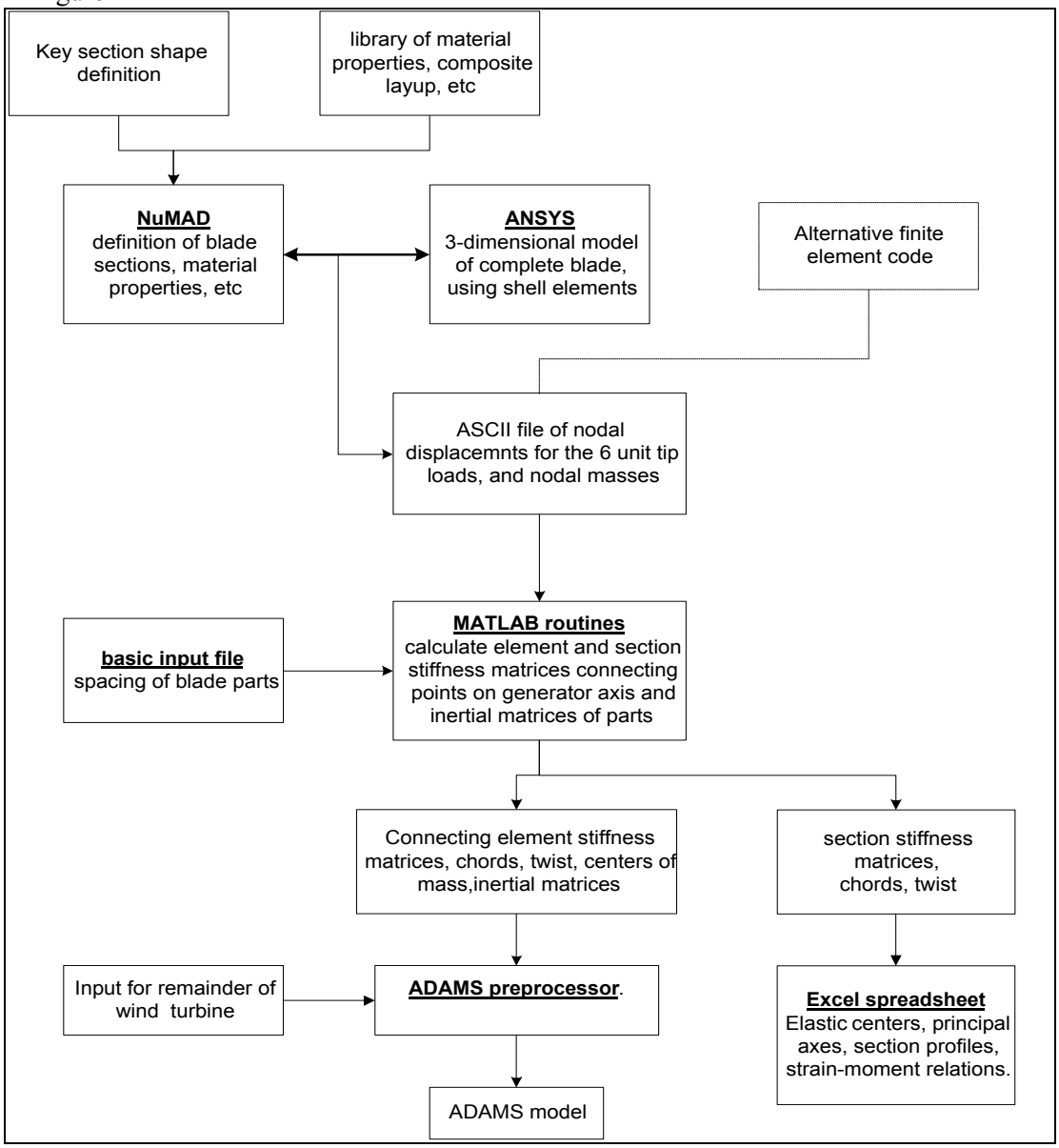

Figure1. Flowchart of overall process

The first step is the creation of a 3-dimensional ANSYS finite element model through the application of the NuMAD interface [Laird, 2001]. This allows the integration of airfoil shapes, spanwise tapering, composite material properties and orientation to generate the final model. This cantilever model is then loaded at the tip by unit forces and moments about the six degrees of freedom and the set of displacements and nodal masses is written to an ASCII file.

The information contained within the six sets of displacements is sufficient to allow extraction of the stiffness matrices relating the sections into which the blade has been divided for the equivalent beam representation. The manner in which this is done is described fully in Appendix A. Appendix B presents the algorithm through which the element stiffness matrix can be used to

derive a "section" stiffness matrix relating the six strains and the six forces or moments at any point or section of the blade. Appendix C shows how the section properties such as elastic and shear centers are extracted from the stiffness matrix.

Validation tests

A number of tests were carried out in the early phases of the work on beams with simple shapes and of isotropic, homogeneous material [GEC, 2001]. The results from these tests showed good agreement with results obtained from classical beam theory so long as the effects of shear deformation were included.

More recent work has focused on validating the suitability of including the stiffness and inertial properties within ADAMS models. These tests included an isotropic constant rectangular section, constant sections corresponding to the 25% and 50% span sections in one of the WindPACT rotor study [GEC, 2002] baseline blades, and a full blade from the same study.

Rectangular section

The dimensions of the test beam are shown in Figure 2. The coordinate origin was offset from the geometric center and the section was rotated 10 degrees relative to the coordinates. This geometry was chosen because it was possible to generate section and beam properties by hand calculations using classical beam theory.

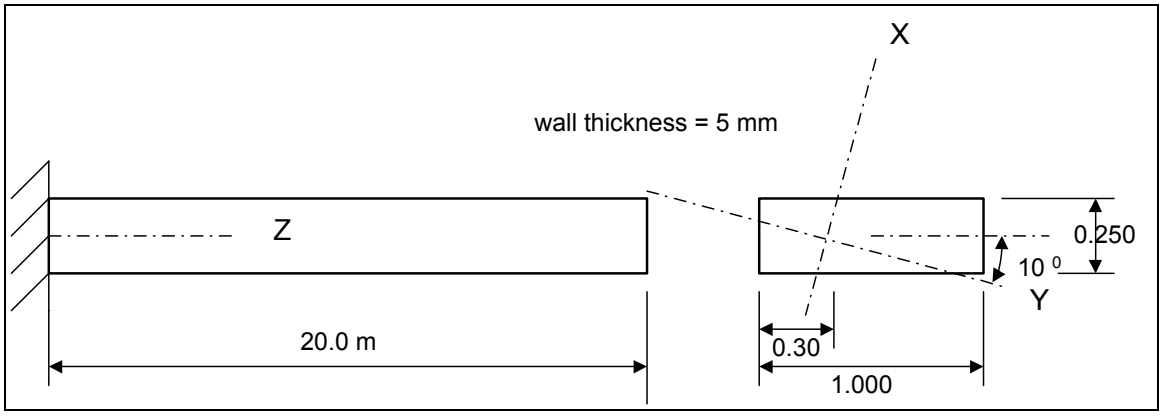

Figure 2. Test beam of rectangular section

An ANSYS finite element model of the beam was generated using the NuMAD interface and used a mesh of 20 elements circumferentially and 50 longitudinally. 8-node quadrilateral composite shell elements were used to describe the structure which was composed of steel with a low Poisson's ratio. For calculation of the equivalent beam properties, the span was divided into 10 equal elements.

The section properties associated with the equivalent beam elements were extracted using the algorithms of Appendix B. From the 6 x 6 stiffness matrix it was possible to calculate characteristics such as the position of the elastic center, the orientation of the principal axes, and the location of the shear center. Table 1 compares the values obtained from the stiffness matrix of the equivalent beam to those obtained from hand calculations.

The stiffness matrices of the equivalent beam elements and the corresponding inertial matrices were incorporated into an ADAMS model of the beam with all terms referenced to one set of coordinates. A unit tip load was applied and the resulting tip displacements were compared with

hand calculations. In addition, the natural frequencies obtained from ADAMS/linear were compared with classical results. The comparisons are included in Table 1.

Table 1. Comparison of deduced and theoretical properties of rectangular section beam

	Equivalent beam	**Theoretical / hand calc.**
Principal major flexural stiffness (N m^2)	290E6	287E6
Principal minor flexural stiffness (N m^2)	32.6E6	32.4E6
Torsional stiffness (N m2)	41.3E6	49.5E6
y-offset to elastic axis (m)	0.197	0.20
y-offset to shear center (m)	0.20	0.20
Major shear stiffness (N)	916E6	495E6
Minor shear stiffness (N)	110E6	247E6
Mass / length (kg/m)	392	392
x-direction tip displacement due to unit x-direction tip load (m)	0.079	0.080
y-direction tip displacement due to unit x-direction tip load (m)	-0.0124	-0.0124
1^{st} flexural natural frequency (Hz)	0.815	0.805
2nd flexural natural frequency (Hz)	2.43	2.40
1^{st} torsional natural frequency (Hz)	24.6	25.9

The flexural stiffness has been defined as the element k_{44} or k_{55} in the section stiffness matrix referred to principal axes passing through the elastic center. This implies that it is the moment required to generate a unit curvature while all other strains are constrained to be zero. In general this is not the same as the classical concept unless there is zero coupling between the rotation applied and other displacements.

The agreement between most of the extracted values and the corresponding classical results is good. Agreement for the shear stiffness is not good; this can be traced to dependence of the shear stiffness on the distribution of shear stress across the section and the assumptions inherent in simple mechanics of material concepts. It is also due to the assumptions within the equivalent beam formulation which must use a least squares best fit to identify the six displacements to describe the deformed section in the finite element model.

Constant section airfoil beams

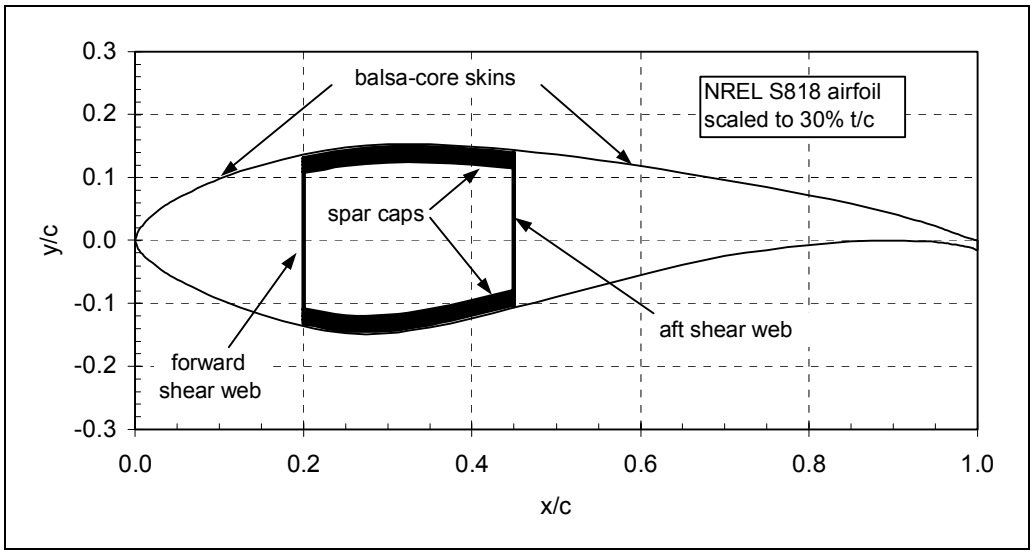

Figure 3. Section of the WindPACT baseline blade at 25% span

Figure 3 shows the section of a blade used in the WindPACT Rotor Design Study [GEC, 2002] at 25% span location. In that study the major section properties were estimated by applying classical beam theory to the various portions and specified materials of the cross section. The same material properties were incorporated into a NuMAD/ANSYS model of a prismatic member which was then converted into equivalent beams elements by the MATLAB procedure. The element and section 6 x 6 stiffness matrices provided all information on the sections, some of which are shown in Table 2 and compared to the earlier WindPACT values. Table 3 shows similar values for the section at 50% span.

Table 2. Comparison of properties extracted from model of 25% span section with WindPACT values

	Equivalent Beam	WindPACT value
Principal major flexural stiffness (N m^2)	6.8E8	6.18E8
Principal minor flexural stiffness (N m^2)	2.73E8	2.72E8
Torsional stiffness (N m^2)	4.07E7	1.88E7
Mass / length (kg/m)	162	185
Elastic axis location from leading edge (fraction of chord)	0.369	0.329
Center of mass location from leading edge (fraction of chord)	0.376	0.410
Orientation of principal axes (degrees clockwise)	-4.0	0.0

Table 3. Comparison of properties extracted from model of 50% span section with WindPACT values

	Equivalent Beam	WindPACT value
Principal major flexural stiffness (N m^2)	2.74E8	2.56E8
Principal minor flexural stiffness (N m^2)	7.42E7	7.52E7
Torsional stiffness (N m^2)	1.18E7	8.48E6
Mass / length (kg/m)	121	138

Elastic axis location from leading edge (fraction of chord)	0.363	0.324
Center of mass location from leading edge (fraction of chord)	0.372	0.386
Orientation of principal axes (degrees clockwise)	-2.9	0.0

The agreement between the extracted properties and the WindPACT values is close except for the torsional stiffness which was known to be underestimated in the WindPACT project.

Full blade model

An illustration of the ANSYS model of the complete blade duplicating the WindPACT baseline 1.5 MW blade is shown in Figure 4. The blade was divided into beam elements of the same length as those used in the WindPACT ADAMS model and the element stiffness and section stiffness matrices were extracted by the MATLAB routines. A comparison of some of the principal properties is given in Table 4 and in Figure 5.

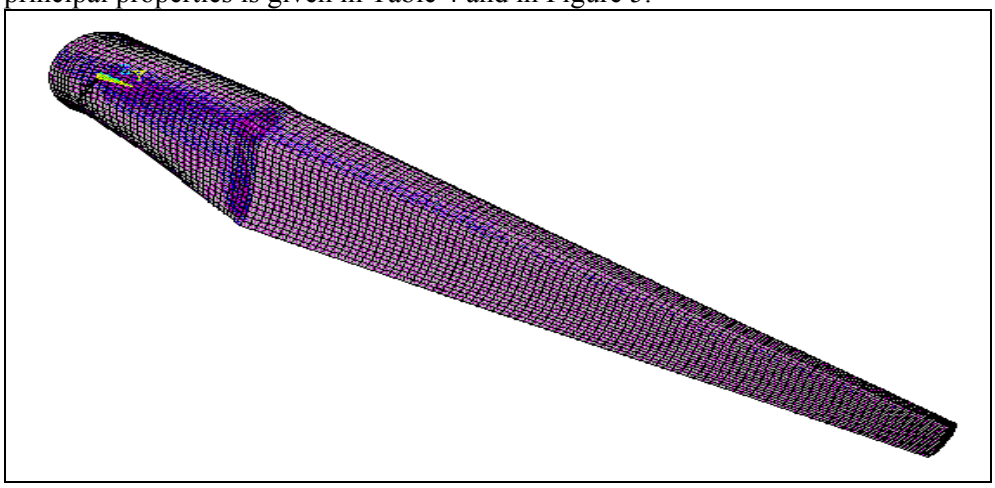

Figure 4. Finite element model of complete blade

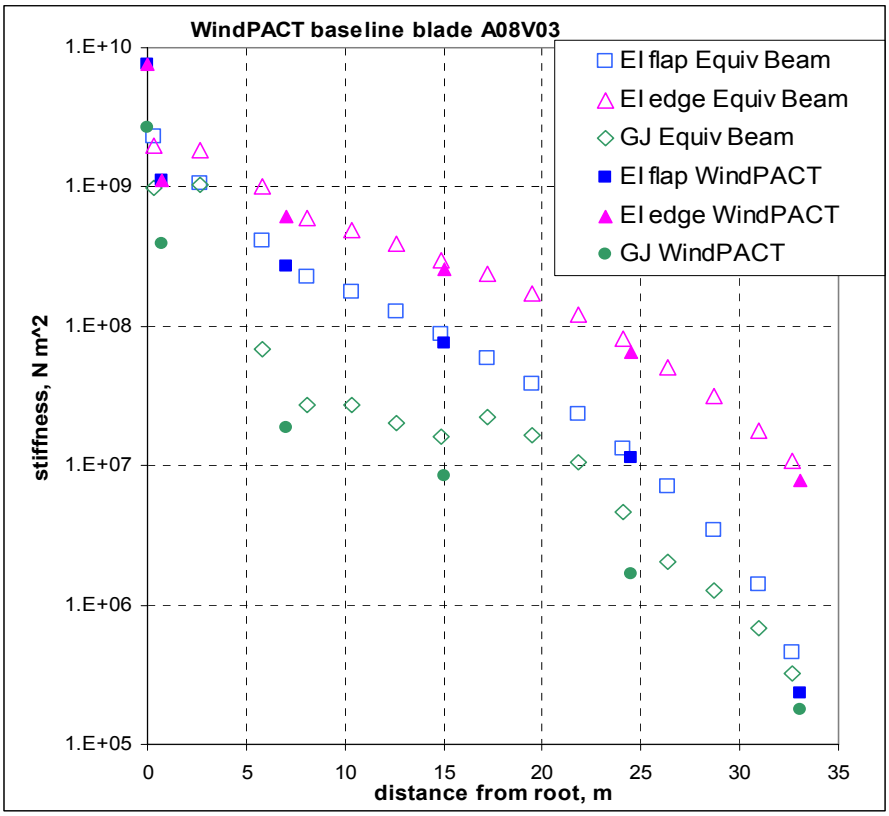

Figure 5. Equivalent Beam estimates and WindPACT values of baseline blade properties

Table 4. Comparison of equivalent beam estimates and WindPACT values

Distance from root (m)	quantity	Equivalent Beam estimate	WindPACT value
0.7 (7% span)	Edgewise flexural stiffness (N m^2)	1.89E9	1.12E9
	Flapwise flexural stiffness (N m^2)	2.10E9	1.12E9
7.0 (25% span)	Edgewise flexural stiffness (N m^2)	7.94E8	6.18E8
	Flapwise flexural stiffness (N m^2)	3.12E8	2.72E8
15.0 (50% span)	Edgewise flexural stiffness (N m^2)	2.99E8	2.56E8
	Flapwise flexural stiffness (N m^2)	8.58E7	7.52E7
24.5 (75% span)	Edgewise flexural stiffness (N m^2)	7.50E7	6.58E7
	Flapwise flexural stiffness (N m^2)	1.22E7	1.15E7
33.2 (100% span)	Edgewise flexural stiffness (N m^2)	9.22E6	7.87E6
	Flapwise flexural stiffness (N m^2)	2.18E5	2.31E5

The values for the equivalent beam estimates in Table 4 have been interpolated or extrapolated in order to be directly comparable to the WindPACT values. This has obscured the trends in regions where the values are changing rapidly, such as at the change of section at z=0.7 m

The WindPACT values were all obtained by applying simple beam theory to each of the four sections while the equivalent beam values reflect the 3-dimensional response of the finite element model. Examination of the deformed ANSYS model showed that in the vicinity of the start and ending of the root taper (between z=0.7 and z=7.0 m) there was considerable distortion of the cross sections which tended to reduce the overall stiffness of the structure. This behavior was traced to inadequate wall thickness in the modeling of the taper and in order to add some internal

stiffening, the webs present in the outboard portions of the blade were extended inwards to the z=0.7 m section.

An ADAMS model of the blade was prepared using the equivalent beam stiffness and inertial properties and the properties of this model were compared with those of the WindPACT baseline blade. This comparison is presented in Table 5.

Table 5. Comparison of ADAMS models of blades from WindPACT and from equivalent beams.

quantity	Equivalent Beam estimate	WindPACT value
x-displacement at tip due to unit x-direction tip load	0.130	0.102
y-displacement at tip due to unit x-direction tip load	-0.0097	-0.0039
x-displacement at tip due to unit y-direction tip load	-0.0097	0.00044
y-displacement at tip due to unit y-direction tip load	0.0304	0.0296
Total mass of blade (kg)	4680	4320
First flapwise natural frequency (Hz)	1.140	1.233
First edgewise natural frequency (Hz)	1.926	1.861
Second flapwise natural frequency (Hz)	3.231	3.650
First torsional natural frequency (Hz)	13.61	9.289

There are some significant differences between the sets of values in Table 5. The difference in total masses is due mainly to differences near the root where the mass of the connection hardware may not have been included fully in the WindPACT model.

The tip displacements and the natural frequencies point to a softer blade from the equivalent beam procedure. This may be due in part to the lower stiffness in the transition region between root and airfoil. It may also be due to the inclusion in the finite element model of shear deformation which was omitted in the conventional procedure used in the WindPACT study. The difference between the torsional natural frequencies is due to the known underestimate of the torsional stiffness in the WindPACT model.

Full turbine models

The blade model from the equivalent beam process was incorporated into a full ADAMS model of the WindPACT baseline turbine. This model was compared with the original WindPACT model by examining the natural frequencies of the stationary turbines and by examining some of the response loads. Table 6 lists some of the natural frequencies.

Table 6. Comparison of full system natural frequencies (Equivalent beam vs. WindPACT model)

Mode #	Mode shape	Equivalent Beam estimate (Hz)	WindPACT value (Hz)
1	Tower lateral	0.368	0.376
2	Tower fore-aft	0.369	0.377
3	Blade flapwise asymmetric, yaw	0.941	0.998

4	Blade flapwise asymmetric, pitch	0.977	1.040
5	Propeller, flapwise collective	1.025	1.086
6	Flapwise collective, propeller	1.124	1.143
7	Blade edgewise asymmetric	1.613	1.595
8	Blade edgewise asymmetric	1.644	1.621
9	2nd flapwise asymmetric, pitch	2.587	2.716
10	2nd flapwise asymmetric, yaw	2.593	2.809

The response of the two wind turbines, as measured by the root flap bending moment, the shaft thrust, the yaw moments, and the tower bending, were in very close agreement.

Summary

The objective of extracting the equivalent beam properties from a 3-dimensional finite element model has been reached. In the course of doing this a number of aspects have been highlighted.

- All structural information can be represented in the beam stiffness matrices referred to the pitch axis coordinates. This includes the location of the elastic axes, orientation of principal aces and all coupling between terms. Warping effects are also captured. This simplifies the aeroelastic modeling.
- Agreement between basic flexural stiffness values obtained by the equivalent beam process and earlier methods for constant airfoil sections is good. Corresponding properties from models of a full blade show more deviation (equivalent beam values are higher).
- Blade models constructed using the equivalent beam method have slightly lower natural frequencies, in apparent contradiction to the previous comment. A reason for this may be the low shear stiffness of the blade material and inclusion of this effect in the equivalent beam method.
- Testing of the equivalent beam method on a rectangular cantilever suggests that this process may underestimate the shear stiffness in the weaker direction and overestimate in the stronger direction. This can be explained by detailed examination of the distorted cross section. Use of a higher order polynomial to fit to the distorted section can correct the results for rectangular sections but more work must be done to validate such an approach for all sections.
- The equivalent beam method show considerable promise for easily including all relevant characteristics into beam elements used for dynamic simulation. This includes incorporation of biased plies to achieve flap-twist coupling in the blade.

References

1. Global Energy Concepts LLC, “Development of blade property extraction code to interface with NuMAD. Phase 1”, submitted to Sandia National Laboratories in response to Document #20173, rev 0, October 2001

2. Global Energy Concepts LLC, “Development of blade property extraction code to interface with NuMAD. Phase 2”, submitted to Sandia National Laboratories in response to Document #20173, rev 0, March 2002.

3. Malcolm, D.J. and Hansen, A.C., “The WindPACT rotor design study”, NREL subcontractors’ review meeting, National Wind Technology Center, Colorado, August 2001.

4. Sihn, S. and Tsai, S.W., "3D Beam manual", Stanford University, Department of Aeronautics and Astronautics.

5. Bir, G, and Migliore, P., "A computerized method for preliminary structural design of composite wind turbine blades", Proceedings of the ASME/AIAA Wind Energy Symposium, Reno, Nevada, January 2001.

6. Laird, D., "A numerical manufacturing and design tool odyssey", Proceedings of the ASME/AIAA Wind Energy Symposium, Reno, Nevada, January 2001.

7. Den Hartog, J.P., "Advanced strength of materials", McGraw Hill, 1952

8. ANSYS Inc., 201 Johnson Road, Houston, PA 15342, 402 746 3304.

9. Malcolm, D.J. and Hansen, A.C., "Lessons from the WindPACT rotor design study," Proceedings of Windpower 2002, AWEA, Portland, June 2002.

10. Global Energy Concepts, LLC, "WindPACT turbine rotor design study, final report," NREL contract YAT-0-30213-01, June 2002.

11. Mechanical Dynamics Inc. (now MSC Software), "ADAMS/Solver reference manual, version 8," November 1994, Ann Arbor, Michigan.

Appendix A Extraction of element stiffness matrices

The general analytical approach is to use a NuMAD/ANSYS finite element model of the blade to provide load and deflection results from a set of linearly independent static load cases. From this information the properties of an equivalent one-dimensional beam are calculated.

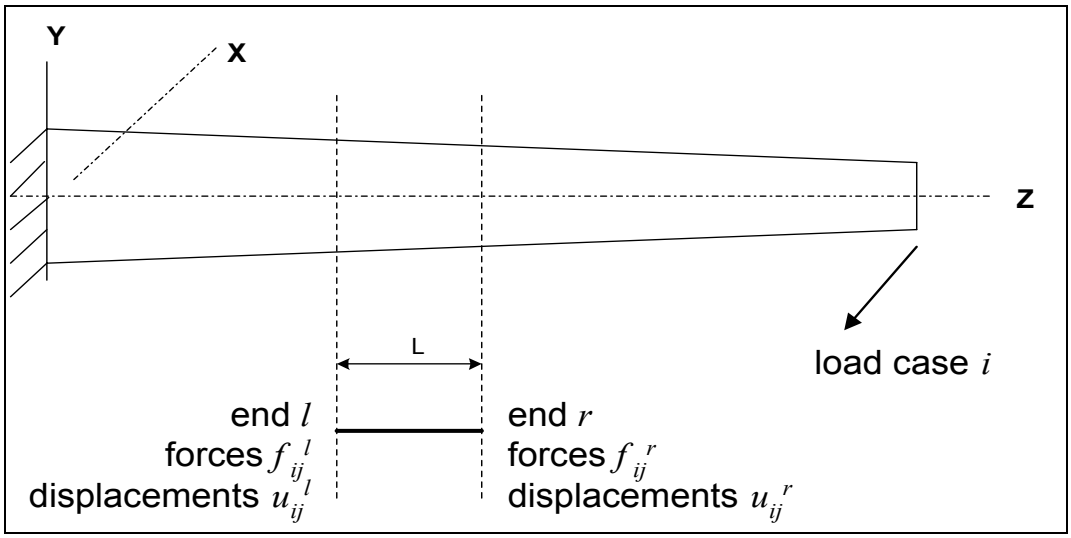

Figure A1. 3-dimensional blade model and equivalent beam element

Each segment of a typical wind turbine blade (see Figure A1) can be treated as an element in a beam model of the blade structure. Any set of static loads on the blade can be resolved, using

only statics, into a set of three forces and three moments internal to the blade on each end of the element. The six forces on the left *l* and right *r* ends of the element for load case *i* can be written as:

$$f_i = \begin{Bmatrix} f_{ij}^l \\ f_{ij}^r \end{Bmatrix}, \quad j = 1,...6. \tag{A1}$$

where $f_{ij}^l = \left\{ f_{ix}{}^l, f_{iy}{}^l, f_{iz}{}^l, M_i x^l, M_{iy}{}^l, M_{iz}{}^l \right\}^T$

Following classical beam theory the deformed element can be described by six displacements at each end (three translations and three rotations) and can be written as

$$u_i = \begin{Bmatrix} u_{ij}^l \\ u_{ij}^r \end{Bmatrix}, \quad j = 1,...6. \tag{A2}$$

where $u_{ij}^l = \left\{ u_{ix}^l, u_{iy}^l, u_{iz}^l, \theta_{ix}^l, \theta_{iy}^l, \theta_{iz}^l \right\}^T$

The displacements and forces are related by a 12x12 stiffness matrix, $\mathbf{K}^{12x12}$.

$$\boldsymbol{K}^{12x12}\{u\} = \{f\}. \tag{A3}$$

Although ADAMS has a finite-element-like formulation, the code describes large displacements and rotations and therefore it defines parts with respect to neighboring parts. Thus, the typical ADAMS implementation uses only one quarter of the full 12x12 stiffness matrix. The quarter used is the one that defines one end of the element with respect to the other, say the right with respect to the left. The displacements are, therefore, relative displacements of the right side with respect to a tangent line at the left end.

$$\begin{aligned}
u_{ix}^{rlx} &= u_{ix}^r - u_{ix}^l - \theta_{iy}^l L \\
u_{iy}^{rl} &= u_{iy}^r - u_{iy}^l + \theta_{ix}^l L \\
u_{iz}^{rl} &= u_{iz}^r - u_{iz}^l \\
\theta_{ix}^{rl} &= \theta_{ix}^r - \theta_{ix}^l \\
\theta_{iy}^{rl} &= \theta_{iy}^r - \theta_{iy}^l \\
\theta_{iz}^{rl} &= \theta_{iz}^r - \theta_{iz}^l
\end{aligned} \tag{A4}$$

where *L* is the length of the element and z is along the axis of the blade.

The resulting 6x6 set of equations depends only on the loads on the right side of the element and has a reduced 6x6 stiffness matrix, ***K*,**

$$\boldsymbol{K}\{u_i\} = \{f_i\} \tag{A5}$$

Each *i* refers to another load case. Therefore, if we can construct six linearly independent load cases we can write a full matrix equation like the following.

$$\begin{aligned}
&\boldsymbol{K}[u_1^{rl} \cdots u_6^{rl}] = [f_1^r \cdots f_6^r] \\
&\text{or} \\
&\boldsymbol{KU} = \boldsymbol{F}
\end{aligned} \tag{A6}$$

Then the solution for ***K*** is obtained as

$$\boldsymbol{K} = \boldsymbol{F}\boldsymbol{U}^{-1} \tag{A7}$$

The inverse of the displacements, U, exists only if the six loads and corresponding displacements are linearly independent. Finding a linearly independent set of load cases is not difficult. For example, tip loads of a unit force or moment in each of the six beam degrees-of-freedom will suffice.

Although there are only six displacements and rotations at each beam node, the NuMAD shell model will have potentially hundreds of degrees-of-freedom at each cross section. There is no unique way to specify the "characteristic" section displacements and rotations. In this work, a least squares algorithm has been used to fit a plane through each deformed cross section, and to infer a single set of displacements and rotations at each section.

Appendix B. Derivation of section stiffness matrix

The stiffness matrix discussed above relates the forces at one end of a beam element to the displacements between the two ends and is of direct use in a code such as ADAMS. However, the element stiffness is a function of the length of that element. The section stiffness is a property at a selected location or section of the blade and relates the six forces at the section to the corresponding six overall strains at the same location. These strains are defined as

$$\{\varepsilon\} = \begin{Bmatrix} \gamma_x \\ \gamma_y \\ \varepsilon_{zz} \\ \kappa_x \\ \kappa_y \\ \kappa_z \end{Bmatrix} = \begin{Bmatrix} \partial u_x / \partial z - \theta_y \\ \partial u_y / \partial z + \theta_x \\ \partial u_z / \partial z \\ \partial \theta_x / \partial z \\ \partial \theta_y / \partial z \\ \partial \theta_z / \partial z \end{Bmatrix} \tag{B1}$$

and the relationship between the internal force resultants, f^z, and the six section strains is

$$\{f^z\} = \begin{Bmatrix} F_x \\ F_y \\ F_z \\ M_x \\ M_y \\ M_z \end{Bmatrix} = [k]\{\varepsilon\} \tag{B2}$$

To obtain the six displacements at end *r* relative to end *l* (see Figure A1), we must integrate the slopes

$$\left\{u^{rl}\right\}=\int_0^L\begin{Bmatrix}\partial u_x/\partial z\\ \partial u_y/\partial z\\ \partial u_z/\partial z\\ \partial\theta_x/\partial z\\ \partial\theta_y/\partial z\\ \partial\theta_z/\partial z\end{Bmatrix}dz=\int_0^L\begin{Bmatrix}\gamma_x+\theta_y\\ \gamma_y-\theta_x\\ \varepsilon_z\\ \kappa_x\\ \kappa_y\\ \kappa_z\end{Bmatrix}dz=\int_0^L[k]^{-1}\left\{f^z\right\}dz+\int_0^L\begin{Bmatrix}\theta_y\\ -\theta_x\\ 0\\ 0\\ 0\\ 0\end{Bmatrix}dz \tag{B3}$$

From statics we can write the section forces, f^z, in terms of the forces at end r, f^r, and the location along the element, z.

$$\left\{f^z\right\}=\begin{bmatrix}1 & & & & & \\ & 1 & & & & \\ & & 1 & & & \\ & & -(L-z) & 1 & & \\ (L-z) & & & & 1 & \\ & & & & & 1\end{bmatrix}\left\{f^r\right\}\equiv[D_z]\left\{f^r\right\} \tag{B4}$$

The second term in Equation (B3) can be written as

$$\begin{Bmatrix}\theta_y\\ -\theta_x\\ 0\\ 0\\ 0\\ 0\end{Bmatrix}=\int_0^z\begin{Bmatrix}\kappa_y\\ -\kappa_x\\ 0\\ 0\\ 0\\ 0\end{Bmatrix}dz=\int_0^z\begin{bmatrix}0 & 0 & 0 & 0 & 1 & 0\\ 0 & & & -1 & & \\ 0 & & & & & \\ 0 & & & & & \\ 0 & & & & & \\ 0 & & & & & \end{bmatrix}\{\varepsilon\}\,dz\equiv\int_0^z[E]\{\varepsilon\}\,dz$$

$$=\int_0^z Ek^{-1}\left\{f^z\right\}dz$$

$$=Ek^{-1}\int_0^z[D_z]\left\{f^r\right\}dz$$

$$=Ek^{-1}\begin{bmatrix}z & & & & & \\ & z & & & & \\ & & z & & & \\ & & -z(L-\frac{z}{2}) & z & & \\ z(L-\frac{z}{2}) & & & & z & \\ & & & & & z\end{bmatrix}f^r$$

$$\equiv Ek^{-1}G_z f^r \tag{B5}$$

Equation (B3) can now be rewritten as

$$\left\{u^{rl}\right\} = k^{-1}\int_0^L D_z f^r dz + Ek^{-1}\int_0^L G_z f^r dz$$

$$= k^{-1}\begin{bmatrix} L & & & & & \\ & L & & & & \\ & & L & & & \\ & -\frac{L^2}{2} & & L & & \\ \frac{L^2}{2} & & & & L & \\ & & & & & L \end{bmatrix} f^r + Ek^{-1}\begin{bmatrix} L^2/2 & & & & & \\ & L^2/2 & & & & \\ & & L^2/2 & & & \\ & -\frac{L^3}{3} & & L^2/2 & & \\ \frac{L^3}{3} & & & & L^2/2 & \\ & & & & & L^2/2 \end{bmatrix} f^r \qquad \text{(B6)}$$

$$\equiv \left(k^{-1}H + Ek^{-1}Q\right) f^r$$

From Equation (A6) we have

$$\left\lfloor u^{rl} \right\rfloor = \left\lfloor K^{-1} \right\rfloor \left\lfloor f^r \right\rfloor \qquad \text{(B7)}$$

where K is the stiffness matrix of the element. From Equations (B6) and (B7) we can write

$$K^{-1} f^r = \left(k^{-1}H + Ek^{-1}Q\right) f^r$$

or

$$K^{-1} = k^{-1}H + Ek^{-1}Q \qquad \text{(B8)}$$

or

$$K^{-1}Q^{-1} = k^{-1}HQ^{-1} + Ek^{-1}$$

The last line of Equation (B8) is in a form that is amenable to solution for k^{-1} using Lyapunov's method. In this way, the section constitutive matrix, k, can be obtained from the element stiffness matrix, K, and the geometry of the element.

Appendix C. Translation and rotation of coordinates

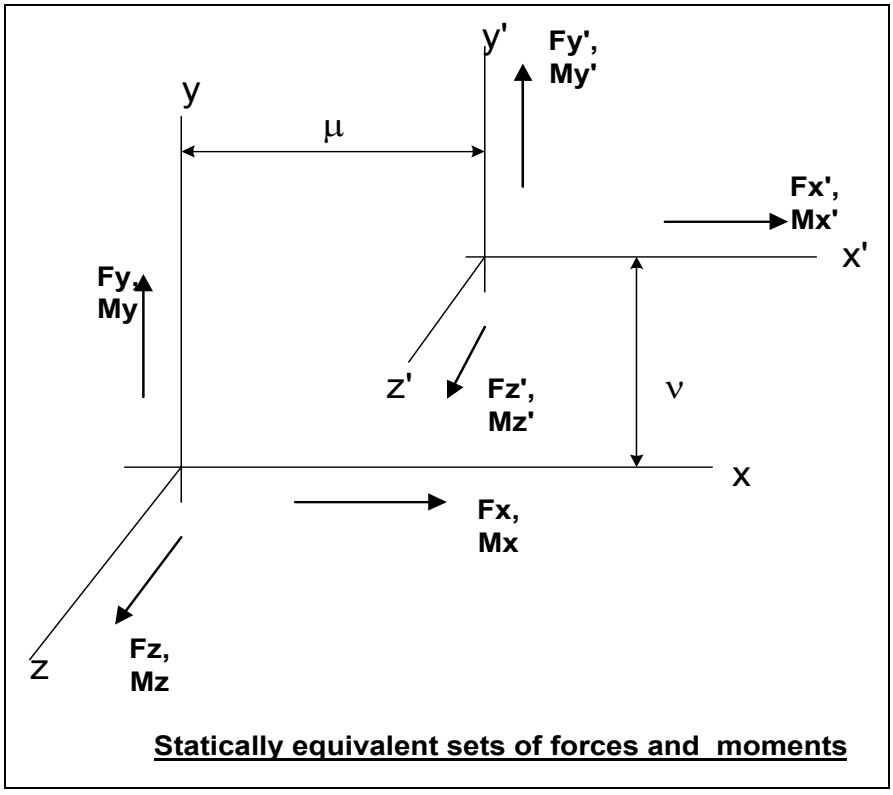

Figure C1. Translation of coordinates

Suppose that the relationship between the six forces/moments and the six strains is known in the xyz coordinate system as:

$$\begin{Bmatrix} F_x \\ F_y \\ F_z \\ M_x \\ M_y \\ M_z \end{Bmatrix} = [k] \begin{Bmatrix} \gamma_x \\ \gamma_y \\ \varepsilon_z \\ \kappa_x \\ \kappa_y \\ \kappa_z \end{Bmatrix} \tag{C1}$$

In terms of the statically equivalent forces and the geometrically equivalent strains in the x'y'z' coordinates (see the Figure C1) this equation becomes

$$\begin{Bmatrix} F_{x'} \\ F_{y'} \\ F_{z'} \\ M_{x'} + \nu F_{z'} \\ M_{y'} - \mu F_{z'} \\ M_{z'} - \nu F_{x'} + \mu F_{y'} \end{Bmatrix} = [k] \begin{Bmatrix} \gamma_{x'} + \nu \kappa_{z'} \\ \gamma_{y'} - \mu \kappa_{z'} \\ \varepsilon_{z'} - \nu \kappa_{x'} + \mu \kappa_{y'} \\ \kappa_{x'} \\ \kappa_{y'} \\ \kappa_{z'} \end{Bmatrix} \tag{C2}$$

By adding and subtracting columns of this equation, we obtain

$$\begin{Bmatrix} F_{x'} \\ F_{y'} \\ F_{z'} \\ M_{x'} + \nu F_{z'} \\ M_{y'} - \mu F_{z'} \\ M_{z'} - \nu F_{x'} + \mu F_{y'} \end{Bmatrix} = \begin{bmatrix} k_{11} & k_{12} & k_{13} & (k_{14} - \nu k_{13}) & (k_{15} + \mu k_{13}) & (k_{16} + \nu k_{11} - \mu k_{12}) \\ k_{21} & \vdots & \vdots & \vdots & \vdots & \vdots \\ k_{31} & \vdots & \vdots & \vdots & \vdots & \vdots \\ k_{41} & \vdots & \vdots & \vdots & \vdots & \vdots \\ k_{51} & \vdots & \vdots & \vdots & \vdots & \vdots \\ k_{61} & k_{62} & k_{63} & (k_{64} - \nu k_{63}) & (k_{65} + \mu k_{63}) & (k_{66} + \nu k_{61} - \mu k_{62}) \end{bmatrix} \begin{Bmatrix} \gamma_{x'} \\ \gamma_{y'} \\ \varepsilon_{z'} \\ \kappa_{x'} \\ \kappa_{y'} \\ \kappa_{z'} \end{Bmatrix} \quad \text{(C3)}$$

Next, by adding and subtracting rows, we obtain

$$\begin{Bmatrix} F_{x'} \\ F_{y'} \\ F_{z'} \\ M_{x'} \\ M_{y'} \\ M_{z'} \end{Bmatrix} = \begin{bmatrix} k_{11} & k_{12} & k_{13} & (k_{14} - \nu k_{13}) & (k_{15} + \mu k_{13}) & (k_{16} + \nu k_{11} - \mu k_{12}) \\ k_{21} & k_{22} & k_{23} & (k_{24} - \nu k_{23}) & (k_{25} + \mu k_{23}) & (k_{26} + \nu k_{21} - \mu k_{22}) \\ k_{31} & k_{32} & k_{33} & (k_{34} - \nu k_{33}) & (k_{35} + \mu k_{33}) & (k_{36} + \nu k_{31} - \mu k_{32}) \\ (k_{41} - \nu k_{31}) & (k_{42} - \nu k_{32}) & (k_{43} - \nu k_{33}) & \begin{pmatrix} k_{44} - \nu k_{43} \\ -\nu(k_{34} - \nu k_{33}) \end{pmatrix} & \begin{pmatrix} k_{45} + \mu k_{43} \\ -\nu(k_{35} + \mu k_{33}) \end{pmatrix} & \begin{pmatrix} k_{46} + \nu k_{41} - \mu k_{42} \\ -\nu(k_{36} + \nu k_{31} - \mu k_{32}) \end{pmatrix} \\ (k_{51} + \mu k_{31}) & (k_{52} + \mu k_{32}) & (k_{53} + \mu k_{33}) & \begin{pmatrix} k_{54} - \nu k_{53} \\ +\mu(k_{34} - \nu k_{33}) \end{pmatrix} & \begin{pmatrix} k_{55} + \mu k_{53} \\ +\mu(k_{35} + \mu k_{33}) \end{pmatrix} & \begin{pmatrix} k_{56} + \nu k_{51} - \mu k_{52} \\ +\mu(k_{36} + \nu k_{31} - \mu k_{32}) \end{pmatrix} \\ \begin{pmatrix} k_{61} + \nu k_{11} \\ -\mu k_{21} \end{pmatrix} & \begin{pmatrix} k_{62} + \nu k_{12} \\ -\mu k_{22} \end{pmatrix} & \begin{pmatrix} k_{63} + \nu k_{13} \\ -\mu k_{23} \end{pmatrix} & \begin{pmatrix} k_{64} - \nu k_{63} \\ +\nu(k_{14} - \nu k_{13}) \\ -\mu(k_{24} - \nu k_{23}) \end{pmatrix} & \begin{pmatrix} k_{65} + \mu k_{63} \\ +\nu(k_{15} + \mu k_{13}) \\ -\mu(k_{25} + \mu k_{23}) \end{pmatrix} & \begin{pmatrix} k_{66} + \nu k_{61} - \mu k_{62} \\ +\nu(k_{16} + \nu k_{11} - \mu k_{12}) \\ -\mu(k_{26} + \nu k_{21} - \mu k_{22}) \end{pmatrix} \end{bmatrix} \begin{Bmatrix} \gamma_{x'} \\ \gamma_{y'} \\ \varepsilon_{z'} \\ \kappa_{x'} \\ \kappa_{y'} \\ \kappa_{z'} \end{Bmatrix} \quad \text{(C4)}$$

Making use of the symmetry of the k matrix, the new equation can be rewritten as

$$\begin{Bmatrix} F_{x'} \\ F_{y'} \\ F_{z'} \\ M_{x'} \\ M_{y'} \\ M_{z'} \end{Bmatrix} = \begin{bmatrix} k_{11} & k_{12} & k_{13} & (k_{14} - \nu k_{13}) & (k_{15} + \mu k_{13}) & (k_{16} + \nu k_{11} - \mu k_{12}) \\ k_{12} & k_{22} & k_{23} & (k_{24} - \nu k_{23}) & (k_{25} + \mu k_{23}) & (k_{26} + \nu k_{12} - \mu k_{22}) \\ k_{13} & k_{23} & k_{33} & (k_{34} - \nu k_{33}) & (k_{35} + \mu k_{33}) & (k_{36} + \nu k_{13} - \mu k_{23}) \\ (k_{14} - \nu k_{13}) & (k_{24} - \nu k_{23}) & (k_{34} - \nu k_{33}) & \begin{pmatrix} k_{44} - 2\nu k_{34} \\ -\nu^2 k_{33} \end{pmatrix} & \begin{pmatrix} k_{45} + \mu k_{34} \\ -\nu(k_{35} + \mu k_{33}) \end{pmatrix} & \begin{pmatrix} k_{46} + \nu k_{14} - \mu k_{24} \\ -\nu(k_{36} + \nu k_{13} - \mu k_{23}) \end{pmatrix} \\ (k_{15} + \mu k_{13}) & (k_{25} + \mu k_{23}) & (k_{35} + \mu k_{33}) & \begin{pmatrix} k_{45} - \nu k_{35} \\ +\mu(k_{34} - \nu k_{33}) \end{pmatrix} & \begin{pmatrix} k_{55} + 2\mu k_{35} \\ +\mu^2 k_{33} \end{pmatrix} & \begin{pmatrix} k_{56} + \nu k_{15} - \mu k_{25} \\ +\mu(k_{36} + \nu k_{13} - \mu k_{23}) \end{pmatrix} \\ \begin{pmatrix} k_{16} + \nu k_{11} \\ -\mu k_{12} \end{pmatrix} & \begin{pmatrix} k_{26} + \nu k_{12} \\ -\mu k_{22} \end{pmatrix} & \begin{pmatrix} k_{36} + \nu k_{13} \\ -\mu k_{23} \end{pmatrix} & \begin{pmatrix} k_{46} - \nu k_{36} \\ +\nu(k_{14} - \nu k_{13}) \\ -\mu(k_{24} - \nu k_{23}) \end{pmatrix} & \begin{pmatrix} k_{56} + \mu k_{36} \\ +\nu(k_{15} + \mu k_{13}) \\ -\mu(k_{25} + \mu k_{23}) \end{pmatrix} & \begin{pmatrix} k_{66} + 2\nu k_{16} - 2\mu k_{26} \\ +\nu^2 k_{11} - 2\nu\mu k_{12} + 2\mu^2 k_{22} \end{pmatrix} \end{bmatrix} \begin{Bmatrix} \gamma_{x'} \\ \gamma_{y'} \\ \varepsilon_{z'} \\ \kappa_{x'} \\ \kappa_{y'} \\ \kappa_{z'} \end{Bmatrix} \quad \text{(C5)}$$

A similar transformation applies to the element stiffness matrix, *K*.

Identification of elastic center

The figure below shows a possible relationship between the axis origin and the elastic axis (offsets μ and ν in the x and y directions respectively).

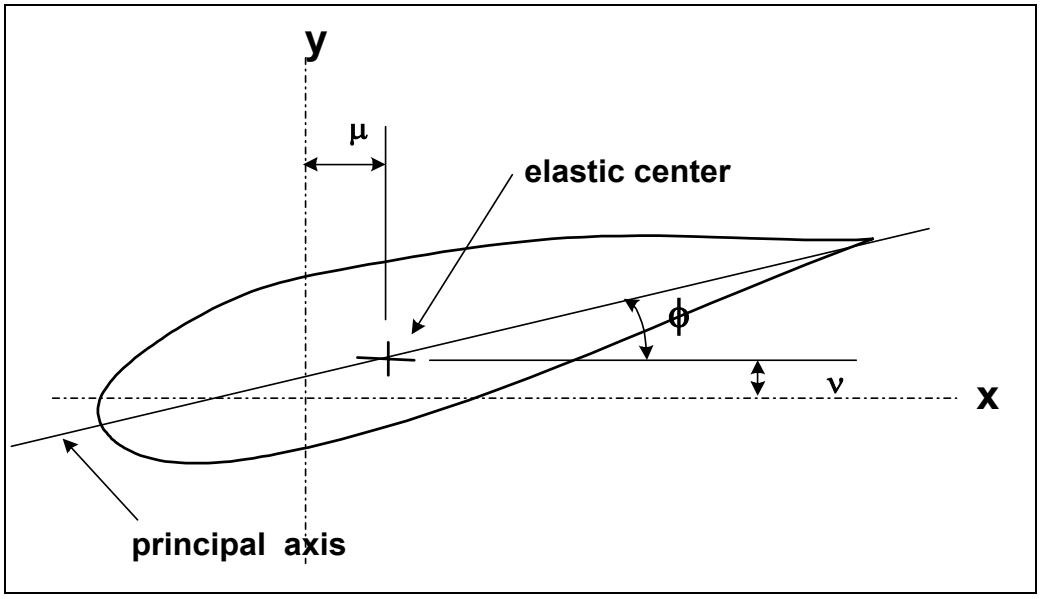

Figure C2. Location of elastic axis and principal axes

We define the elastic center as the location on the cross section with the following properties: the imposition of an axial strain, ε_z, (while other strains are zero) can be maintained by an axial force, F_z, through the elastic center and zero additional moments about the x and y axes. This may be expressed as

$$\begin{aligned} F_z &= k_{33}\varepsilon_z \\ M_x &= F_z\nu = k_{43}\varepsilon_z \\ M_y &= -F_z\mu = k_{53}\varepsilon_z \end{aligned} \qquad \text{(C6)}$$

from which it follows that

$$\begin{aligned} \nu &= {}^{k_{43}}\!/_{k_{33}} \\ \mu &= -{}^{k_{53}}\!/_{k_{33}} \end{aligned} \qquad \text{(C7)}$$

Note that use of this definition implies that transfer of the axes origin to the elastic center will result in zero coupling between axial strain and curvatures (i.e. $k_{43} = 0$, $k_{53} = 0$). It does not imply that $k_{13} = 0$, or $k_{23} = 0$. In general the application of an axial strain, ε_z, will result in lateral forces, F_x and F_y, to ensure that shear strains, γ_x and γ_y, remain zero.

The above definition of the elastic axis is not identical to that defined by applying an axial force and requiring that all other forces be zero. This alternative definition leads to zero coupling terms in the flexibility matrix (the inverse to the stiffness matrix).

Rotation to principal axes

We define a principal axis as a direction about which an applied curvature will result in a moment about that axis and zero moment about the perpendicular axis. Using the transformation due to a rotation, φ,

$$\mathrm{K'} = \mathrm{RKR}^{\mathrm{T}} \quad \text{where} \quad \mathrm{R} = \begin{bmatrix} \cos\phi & \sin\phi & 0 \\ -\sin\phi\cos\phi & 0 \\ 0 & 0 & 1 \end{bmatrix} \qquad \text{(C8)}$$

results in a term

$$k'_{45} = k_{45}(\cos^2\phi - \sin^2\phi) + (k_{55} - k_{44})\sin\phi\cos\phi \,. \quad \text{(C9)}$$

For the left hand side of this equation to be zero it is necessary that

$$\tan 2\phi = \frac{2k_{45}}{k_{44} - k_{55}} \quad \text{(C10)}$$

Note that Equation (C10) does not imply that a lateral shear strain along a principal axis will result in a lateral force in that direction only; nor does it imply that a lateral shear strain will result in moments about the corresponding axis only.

Identification of shear center

We define the shear center as a location on the cross section with the following properties: we impose a lateral strain, γ_x, while all other strains are restrained to be zero and we suppose that these restraints include a lateral force, F_x, through the shear center but zero additional torque, M_z. Then we can write

$$\begin{aligned} F_x &= k_{11}\gamma_x \\ M_z &= -F_x\nu = k_{61}\gamma_x \end{aligned} \quad \text{(C11)}$$

Combining these two equations, we obtain

$$\nu = \frac{-k_{61}}{k_{11}} \,. \quad \text{(C12)}$$

Similarly we may show

$$\mu = \frac{k_{62}}{k_{22}} \,. \quad \text{(C13)}$$

If the origin of the axes is transformed to the shear center, then there will be zero coupling, k_{16} and k_{26}, between torque and lateral strains. As with the elastic center, this definition is not, in general, identical to one which considers an applied lateral force through the shear center, while all other forces are zero, to result in zero twist. This alternative definition will result in zero coupling terms in the flexibility matrix but not in the stiffness matrix.